Meteorological drought in semi-arid regions: A case study of Iran

Hushiar HAMARASH[1*], Rahel HAMAD[1], Azad RASUL[2]

[1] Scientific Research Center, Soran University, Soran 44008, Iraq;
[2] Faculty of Arts, Department of Geography, Soran University, Soran 44008, Iraq

Abstract: Drought occurs in almost all climate zones and is characterized by prolonged water deficiency due to unbalanced demand and supply of water, persistent insufficient precipitation, lack of moisture, and high evapotranspiration. Drought caused by insufficient precipitation is a temporary and recurring meteorological event. Precipitation in semi-arid regions is different from that in other regions, ranging from 50 to 750 mm. In general, the semi-arid regions in the west and north of Iran received more precipitation than those in the east and south. The Terrestrial Climate (TerraClimate) data, including monthly precipitation, minimum temperature, maximum temperature, potential evapotranspiration, and the Palmer Drought Severity Index (PDSI) developed by the University of Idaho, were used in this study. The PDSI data was directly obtained from the Google Earth Engine platform. The Standardized Precipitation Index (SPI) and the Standardized Precipitation Evapotranspiration Index (SPEI) on two different scales were calculated in time series and also both SPI and SPEI were shown in spatial distribution maps. The result showed that normal conditions were a common occurrence in the semi-arid regions of Iran over the majority of years from 2000 to 2020, according to a spatiotemporal study of the SPI at 3-month and 12-month time scales as well as the SPEI at 3-month and 12-month time scales. Moreover, the PDSI detected extreme dry years during 2000–2003 and in 2007, 2014, and 2018. In many semi-arid regions of Iran, the SPI at 3-month time scale is higher than the SPEI at 3-month time scale in 2000, 2008, 2014, 2015, and 2018. In general, this study concluded that the semi-arid regions underwent normal weather conditions from 2000 to 2020. In a way, moderate, severe, and extreme dry occurred with a lesser percentage, gradually decreasing. According to the PDSI, during 2000–2003 and 2007–2014, extreme dry struck practically all hot semi-arid regions of Iran. Several parts of the cold semi-arid regions, on the other hand, only experienced moderate to severe dry from 2000 to 2003, except for the eastern areas and wetter regions. The significance of this study is the determination of the spatiotemporal distribution of meteorological drought in semi-arid regions of Iran using strongly validated data from TerraClimate.

Keywords: meteorological drought; precipitation; Standardized Precipitation Index; Standardized Precipitation Evapotranspiration Index; Palmer Drought Severity Index; Iran

Citation: Hushiar HAMARASH, Rahel HAMAD, Azad RASUL. 2022. Meteorological drought in semi-arid regions: A case study of Iran. Journal of Arid Land, 14(11): 1212–1233. https://doi.org/10.1007/s40333-022-0106-9

1 Introduction

Drought occurs in almost all climate zones and is considered a major natural hazard (Zhang et al., 2019). Drought is characterized by prolonged water deficiency due to unbalanced demand and

*Corresponding author: Hushiar HAMARASH (E-mail: hrh670h@src.soran.edu.iq)
Received 2022-06-26; revised 2022-10-11; accepted 2022-10-22

supply of water (Zhou et al., 2022), persistent insufficient precipitation, lack of moisture, and high evapotranspiration (Yang et al., 2018), drought from lack of precipitation, which is a transient and recurring meteorological event (Beyaztas et al., 2018). Drought is an uncertain natural phenomenon with an undefined onset. It is the most destructive natural occurrence on the planet, with global consequences, not only in regions with low average rainfall. In other words, drought is an inescapable recurring event that annually affects more than half of the world. Unlike other environmental disasters, their onset and progression are unnoticeable and gradual, albeit having cumulative and catastrophic impacts (Hamarash et al., 2022). Drought is classified into four types: meteorological (lack of precipitation), hydrological (deficiency in surface or subsurface streamflow), agricultural (deficiencies of soil moisture), and socioeconomic (inability to meet water resource demand) drought (Wang et al., 2019).

Droughts are observable after a prolonged time of no precipitation, but their beginning, extent, and end are difficult to be predicted. Despite, their characteristics in terms of intensity, magnitude, persistence, and spatial extent are complicated. Hence, a lot of effort has been spent on developing drought analysis and monitoring methods (Vicente-Serrano et al., 2010). The first and most important issue we face when studying drought is that determine the drought indices. However, drought indices have been still discovered and examined that can be used across different climate zones and at various time scales (Wang et al., 2019). To date, there have been a vast number of meteorological drought indices. The Palmer Drought Severity Index (PDSI), Standardized Precipitation Index (SPI), Effective Drought Index (EDI), Reconnaissance Drought Index (RDI), and the Standardized Precipitation Evapotranspiration Index (SPEI) are the most widely utilized indices. Since drought threats are so complex, no single drought index is appropriate for all places or tasks. To analyze the sensitivity and accuracy of indices, it is critical and effective to consider more than one index (Banimahd and Khalili, 2013). Moreover, the SPI is primarily based on precipitation, is simple to compute, and has multi-scalar properties that distinguish between different types of droughts. The PDSI is based on soil water balance and requires quite high range of data. It cannot also respond to the basic multi-scalar nature of drought. The SPEI is based on a climatic water balance (the difference between precipitation (P) and evapotranspiration (ET)) calculated monthly (or weekly). The SPEI integrates the SPI's multi-scalar characteristics and straightforward calculation with the PDSI's sensitivity to changes in evaporation requirements, which induces by temperature variation and trends; the SPEI's key advantage is the flexibility to distinguish between various drought conditions. Therefore, this advantage can be used to monitor and investigate drought features in the context of global warming (Tan et al, 2015). Furthermore, the reasons for using these indices (SPI and SPEI) in this study are that they have a priority for detecting drought over various time scales, ranging from 3, 6, 9, 12, and 24 to 48 months. On the one hand, the SPI is widely employed all over the world because it only depends on precipitation data (Kazemzadeh and Malekian, 2016; Nasrollahi et al., 2018). On the other hand, the SPEI outperforms other indices in evaluating drought characteristics, particularly in regions with humid, hyper-arid, semi-arid, and Mediterranean climates (Zarei et al., 2021).

The University of Idaho established Terrestrial Climate (TerraClimate) as a high-resolution dataset of monthly climate and climatic water balance for worldwide terrestrial surfaces. It provides a global monthly precipitation time series from 1958 to the present (Hamed et al., 2021). Furthermore, TerraClimate can provide long-term monthly precipitation data for drought hazard assessment (Salvacion, 2022). It is thought that precipitation data from remote sensing products, especially TerraClimate, might be an option for solving the problem of semi-arid water balance due to a combination of rainfall measured at rain gauge stations and actual evapotranspiration from satellite products, such as moderate-resolution imaging spectroradiometer (MODIS) Global Terrestrial Evapotranspiration Product (MOD16) and the Global Land Evaporation and Amsterdam Model (GLEAM). The examination of these products is particularly essential since the information from remote sensing and spatial databases can lead to the process of collecting more realistic hydrological variables (Neto et al., 2022). According to Hamed et al. (2021), TerraClimate has the best performance in South Egypt, against gauge records, compared to the

other products such as Global Land Data Assimilation System (GLDAS)-Noah Model, European Reanalysis (ERA5), and Climatologies at high resolution for the Earth's land surface areas (CHELSA). Another study conducted by Araneda et al. (2020) assessed the TerraClimate datasets as alternative data sources for in situ measurements of hydrometeorological variables and proved that TerraClimate products are an appropriate complementary data source. In addition, TerraClimate products are the best in terms of estimating the spatial distribution and long-term mean actual evapotranspiration (Huerta et al., 2020). TerraClimate products can be used as a substitute for ground data where the data is difficult to obtain.

Many studies investigate drought based on indices, but few studies rely solely on TerraClimate. Therefore, in this regard, the objectives of this study are to evaluate spatiotemporal distribution of meteorological drought conditions in Iran and to assess drought in semi-arid regions using the reliable data of TerraClimate. Furthermore, the reasons that TerraClimate is used in this study are that it is a well-known dataset that provides monthly climate and climatic water balance for global terrestrial surfaces since 1958, has strong validation with station-based observations, and provides data on a global scale with high spatial resolution and time-varying data (Abatzoglou, 2021). The novel contribution of this study is the determination of the spatiotemporal distribution of meteorological drought in semi-arid regions of Iran using validated data from TerraClimate.

2 Materials and methods

2.1 Study area

According to the Köppen climate classification, Iran has both cold and hot semi-arid regions, covering a large area. Iran is considered the largest semi-arid region in the world with a geographical position of 25°N–40°N and 45°E–60°E. It consists of two different climate semi-arid zones, which are known as cold and hot semi-arid regions. It stretches from the Bushehr Province in the southwest to the North Khorasan Province in the northeast, and from the small parts of Sistan and Baluchestan Province in the southeast to the Kermanshah Province in the northwest. Most importantly, while province's names are used in this study, however, they may include small portions located in semi-arid regions, such as Ilam, Esfahan, Qom, Sistan and Baluchestan, and Kurdistan provinces or might the entire provinces have been considered as semi-arid provinces such as Razavi Khorasan, South Khorasan, Yazd, and Kerman provinces. It was found that semi-arid regions were different in the literature (Rahimi and Laux, 2020). In this study, we used climate maps of Iran to extract semi-arid regions based on Peel et al. (2007).

2.2 Precipitation

Precipitation in semi-arid regions is different from other regions, which ranges between 50 and 750 mm. In general, the western and northern semi-arid regions of Iran received more precipitation than the east and south (Fig. 1). From 2000 to 2014, annually total precipitation ranged from 50 to 250 mm in the southeast and central semi-arid region. In contrast, precipitation was higher in the north, northwest, and southwest compared to other parts. Annually total precipitation was between 300 and 550 mm from 2000 to 2014. More precipitation fell in Northwest and South Iran in 2018 and 2019, respectively. The wettest year is 2019 for the entire region. A previous study has shown a similar trend in the amount of precipitation in the semi-arid region with an average annual precipitation of 250 mm (Zoljoodi and Didevarasl, 2013).

2.3 Data sources

The following variables were used in this study: monthly precipitation, minimum temperature, maximum temperature, evapotranspiration, and the PDSI. These data were obtained from TerraClimate product, which developed by the University of Idaho on the Google Earth Engine platform. Table 1 provided the characteristics of TerraClimate dataset with their temporal and spatial resolution. In this study, the nearest neighbor method was used to resample the data resolution to spatial resolution of 1 km, the time resolution was monthly as it was provided by

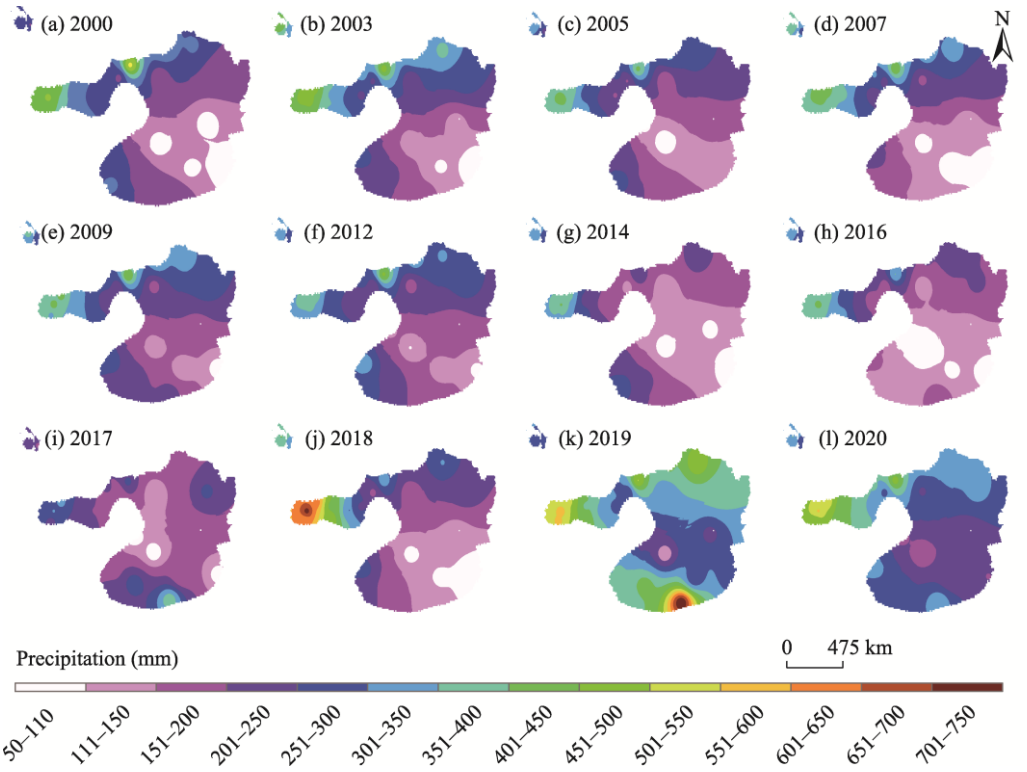

Fig. 1 Spatiotemporal distribution of precipitation in semi-arid regions of Iran in 2000 (a), 2003 (b), 2005 (c), 2007 (d), 2009 (e), 2012 (f), 2014 (g), 2016 (h), 2017 (i), 2018 (j), 2019 (k), and 2020 (l)

Table 1 Characteristics of Terrestrial Climate (TerraClimate)

Variable	Dataset	Spatial resolution	Temporal resolution
Maximum temperature (°C)	WorldClim V1.4 and CRU TS4.0	1/24° and 0.50°	Monthly
Minimum temperature (°C)	WorldClim V1.4 and CRU TS4.0	1/24° and 0.50°	Monthly
Precipitation accumulation (mm)	WorldClim V2.0, CRU TS4.0, and JRA-55	1/24°, 0.50°, and 1.25°	Monthly
Wind speed at 10 m (m/s)	WorldClim V2.0 and JRA-55	1/24°	Monthly
Vapor pressure at 2 m (kPa)	WorldClim V2.0, CRU TS4.0, and JRA-55	1/24°, 0.50°, and 1.25°	Monthly
Vapor pressure deficit (kPa)	Root zone storage capacity	4638.3 m	Time invariant
Snow water equivalent (mm)	-	4638.3 m	Time invariant
Downward shortwave radiation flux at the surface (W/m^2)	WorldClim V2.0 and JRA-55	1/24° and 1.25°	Monthly
Soil moisture (mm)	Root zone storage capacity	4638.3 m	Time invariant
Runoff (mm)	-	4638.3 m	Time invariant
Reference evapotranspiration (mm)	-	4638.3 m	Time invariant
Climate water deficit (mm)	-	4638.3 m	Time invariant
Palmer Drought Severity Index	-	4638.3 m	Time invariant
Actual evapotranspiration (mm)	-	4638.3 m	Time invariant

Note: CRU TS4.0, Climate Research Unit time series data version 4.0; JRA-55, the Japanese 55-year reanalysis. "-" indicates no data. All the information is based on Abatzoglou et al. (2018a, b, 2021) and Abdelmigid et al. (2022).

TerraClimate product. In addition, TerraClimate is a monthly-timestep worldwide gridded dataset of meteorological and water balance indicators from 1958 to the present. Its fine spatial resolution, worldwide range, and extended length make it a one-of-a-kind dataset that fills a gap in climate data. TerraClimate uses climatically aided interpolation, combining high-spatial

resolution climatological normals from the WorldClim dataset with Climate Research Unit time series data version 4.0 (CRU TS4.0) coarser resolution time-varying information and the Japanese 55-year reanalysis (JRA-55) (Abatzoglou et al., 2018a). For most worldwide land surfaces, temporal data of temperature, precipitation, and evapotranspiration is acquired from CRU TS4.0. On the other hand, JRA-55 data is used in geographic areas where Climate Research Unit (CRU) data had no climate stations contributing (including all of Antarctica, parts of Africa, parts of South America, and scattered islands). In addition, TerraClimate is a worldwide database that has been successfully utilized in previous drought analyses, and TerraClimate products are demonstrated to be excellent complementary data sources (Araneda et al., 2020), which have the highest and greatest spatial resolutions (Neto et al., 2022) and assess the spatial distribution of actual evapotranspiration extremely well (Huerta et al., 2020).

2.4 Methods

Drought is a multi-scalar occurrence. Hence, three well-known indices (PDSI, SPEI, and SPI) are used for monitoring meteorological drought in semi-arid regions of Iran. The SPI is generally recognized because it can be calculated at various timescales to monitor droughts concerning specific water resources. The SPI is a precipitation-based index that is calculated using the precipitation over a certain region (McKee et al., 1993). The SPEI is established to monitor drought. It is related to the SPI but includes calculations of moisture losses to the atmosphere due to evapotranspiration. The SPEI is determined at various time scales depending on precipitation and potential evapotranspiration changes (Vicente-Serrano et al., 2010). They are prioritized for drought detection over a variety of time periods, including 3, 6, 9, 12, 24, and 48 months. The PDSI requires a lot of data and is based on soil water balance. Additionally, it is unable to react to drought's fundamental multi-scalar characteristics. The important variable of PDSI is weather data, which is helpful to diagnose long-term drought. The PDSI is developed to manage drought in semi-arid and dry sub-humid regions. This climatic analysis approach must be considered while measuring and describing meteorological drought (Palmer, 1965).

2.4.1 Palmer Drought Severity Index (PDSI)

The PDSI data was obtained from the Google Earth Engine platform. The PDSI is one of the most well-known and commonly used drought indices (Palmer, 1965). The PDSI requires monthly or weekly mean temperatures, total precipitation, soil moisture content, for example, available water holding capacity, and potential evapotranspiration amounts for obtaining the soil moisture balance algorithm. Potential evapotranspiration and latitude are required for the PDSI (Tatli and Türkeş, 2011). In addition, the PDSI was initially not contained in the TerraClimate dataset but was afterward added (see http://www.climatologylab.org/TerraClimate.html). The PDSI from TerraClimate employs Palmer's standard approach (Palmer, 1965), which uses both reference evapotranspiration and monthly precipitation in the PDSI calculation (Kodandapani and Parks, 2019). As a result, in addition to precipitation data and potential evapotranspiration values, the soil's water holding capacity must be provided for the calculation of PDSI. The soil's water holding capacity is present in soil moisture storage, which is divided into two layers. The upper layer is assumed to hold 25.4 mm of available water holding capacity at the field capacity, and the underlying layer holds available water holding capacity differently depending on the soil characteristics (Tall, 2008). Hence, the PDSI can be used to monitor long-term meteorological droughts.

2.4.2 Standard Precipitation Index (SPI)

The SPI was generally introduced to detect dry and wet periods. Also, the SPI is an optimum index for monitoring drought at different time scales from 1 month to 24 months, which was developed by McKee et al. (1993) and recommended as a standard drought index by the World Meteorological Organization. Only precipitation data for about 20 years or more is required to show dry and wet conditions (Tan et al., 2015). In this study, monthly precipitation data during 2000–2020 is employed to calculate the monthly SPI values for semi-arid regions in Iran.

We can determine the SPI for any place based on long-term precipitation records for the selected period. The long-term data is fitted to a gamma probability distribution, which is then transformed into a normal distribution, yielding a zero-mean SPI for the given location and period. Below-average and above-average precipitation are indicated by the negative and positive SPI values, respectively. Dryness is indicated by precipitation below the median, whereas wetness is indicated by precipitation above the median. As a result, the SPI equation can be used to evaluate and track both wet and dry periods in a given area (Tefera et al., 2019). The gamma probability density function was first used for a specific frequency distribution of precipitation data in the proposal of McKee et al. (1993), which was utilized to measure climate and drought change. A gamma distribution is frequently employed to describe temporally averaged precipitation statistics (Martinez-Villalobos and Neelin, 2019; Liu et al., 2021). The calculated process is as follows:

$$p(x) = \frac{1}{\beta^{\alpha}\Gamma(\alpha)} x^{\alpha-1} \exp\left(-\frac{x}{\beta}\right), \tag{1}$$

$$\Gamma(\alpha) = \int_0^{\infty} x^{\alpha-1} \exp(-x)\mathrm{d}x\,, \tag{2}$$

$$\mathrm{SPI} = \frac{(x_i - \bar{x})}{\sigma}, \tag{3}$$

where $p(x)$ is the gamma probability density function to a given frequency distribution of precipitation; α is a shape parameter (α>0); β is a scale parameter (β>0); x is the amount of precipitation (x>0; mm); $\Gamma(\alpha)$ is the gamma function; SPI is the Standardized Precipitation Index; x_i is rainfall in year i; $\bar{x}$ is long-term average rainfall; and σ is the standard deviation.

The SPI can be calculated for any duration from 1 month to 24 months depending on research interest; a time scale of 1 month to 3 months is capable to show meteorological drought; a time scale of 6 months is appropriate to agricultural drought; and more than 6 months is suitable for hydrological drought, which reveals any shortage of groundwater, reservoir, and streamflow water and illustrates soil moisture conditions due to the lack of precipitation (Tefera et al., 2019).

2.4.3 Standardized Precipitation Evapotranspiration Index (SPEI)

Vicente-Serrano et al. (2010) introduced the SPEI as a drought index that is responsive to both precipitation and air evaporative demand and can be estimated on various time scales. The SPEI enhanced the commonly used SPI, which may be calculated using simple precipitation data. Monthly potential evapotranspiration was calculated according to the Food and Agriculture Organization-56 Penman-Monteith method, which allows the SPEI to achieve excellent outcomes regarding drought, streamflow, and soil moisture monitoring (Zhang et al., 2018). As shown in Table 2, there are two values to represent dry and wet conditions, with negative values representing dry conditions, positive values representing wet conditions.

Table 2 Range of the Standard Precipitation Index (SPI) and the Standardized Precipitation Evapotranspiration Index (SPEI) for drought

Range	Class
≥2.00	Extreme wet
1.50–1.99	Severe wet
1.00–1.49	Moderate wet
–0.99–0.99	Near normal
–1.00– –1.49	Moderate dry
–1.50– –1.99	Severe dry
≤ –2.00	Extreme dry

Reference evapotranspiration was calculated using the Penman-Monteith approach (Allen et al., 1998), the calculated equation is as follows:

$$\mathrm{ET}_0 = \frac{0.468\Delta(R_n - G) + \gamma \frac{900}{T+237} U_2 (e_s - e_a)}{\Delta + \gamma(1 + 0.34U_2)}, \quad (4)$$

where ET_0 is reference evapotranspiration (mm/d); Δ is the slope of saturation vapour pressure curve (kPa/°C); R_n is net radiation at the crop surface (MJ/(m^2·d)); G is soil heat flux density (MJ/(m^2·d)); T is mean daily air temperature at 2 m height (°C); U_2 is wind speed at 2 m height (m/s); e_s is saturation vapour pressure (kPa); e_a is actual vapour pressure (kPa); and γ is psychrometric constant (kPa/°C).

The estimation of monthly potential evapotranspiration is the first step in the calculation of SPEI. Then, we calculated the monthly deficit of potential evapotranspiration based on the water balance equation:

$$D_i = P_i - \mathrm{PET}_i, \quad (5)$$

where D_i is the moisture deficit in month i from the monthly difference between the precipitation and the PET; P_i is the precipitation in month i (mm); and PET_i is the potential evapotranspiration in month i (mm).

The values of monthly deficit of potential evapotranspiration are aggregated at different time scales as follows:

$$D_n^k = \sum_{i-0}^{k-1} P_{n-1} - (\mathrm{PET})_{n-1}, \quad (6)$$

where D is the moisture deficit (mm); k is the timescale of the aggregation; n is the calculation month; i is a given month; P is precipitation (mm); and PET is the potential evapotranspiration (mm).

The difference in the water balance is normalized as a log-logistic probability distribution to determine the value of SPEI. The probability density function is expressed by the following equation:

$$f(x) = \frac{\beta}{\alpha}\left(\frac{x-y}{\alpha}\right)\left[1 + \left(\frac{x-y}{\alpha}\right)\right]^{-2}, \quad (7)$$

where $f(x)$ is the probability density function of a three-parameter log-logistic distributed variable; and y is an origin parameter (y>D). Therefore, the probability distribution function can be expressed as:

$$F(x) = \left[1 + \left(\frac{\alpha}{x-y}\right)^{\beta}\right]^{-1}, \quad (8)$$

where $F(x)$ is the cumulative distribution function of the D values.

$$\mathrm{SPEI} = W - \frac{C_0 + C_1 W + C_2 W^2}{1 + d_1 W + d_2 W^2 + d_3 W^3}, \quad (9)$$

where SPEI is the Standardized Precipitation Evapotranspiration Index; C_0, C_1, C_2, d_1, d_2, and d_3 are constant (C_0=2.515517, C_1=0.802285, C_2=0.010328, d_1=1.432788, d_2=0.189269, and d_3=0.001308); and W is probability-weighted moments.

2.4.4 Spatial distribution analysis

The inverse distance weighting method was used to estimate both SPI and SPEI distributions spatially and temporally. The inverse distance weighting method can be used for multivariate interpolation. The idea of inverse distance weighting depends on the assumption that an un-sampled point's attribute value is the weighted average of known values in the area. This is the technique of using values from a distributed set of known points to assign values to unknown points. The weighted sum of the values of known points is the value at the unknown point. The inverse distance weighting is a deterministic method for multivariate interpolation (Chen and Liu, 2012). The inverse distance weighting method, which is based on the concept of distance

weighting, is utilized to interpolate spatial data in this study.

The inverse distance weighting method, also known as inverse distance-based weighted interpolation, uses a weighted mean of adjacent observations to estimate the known value at point *x*. The calculated equation is as follows:

$$Z(x)=\frac{\sum_i^m w_i z}{\sum_i^m w_i}, \tag{10}$$

where $Z(x)$ is the predicted value at location *x*; *z* is known value; w_i is the weighting of each point value; *m* is the number of nearest known points surrounding location *x*.

$$w_i=(x-x_i)^{-\beta}, \tag{11}$$

where *x* is an interpolated and arbitrary point; and x_i is an interpolated and known point. β greater than 0 corresponds to the Euclidean distance. The inverse distance determines the degree to which the nearer points are preferred over more distant points. The number of surrounding points decides whether a global or local weighting is applied. If the point coincides with an observation location, then the observed value is returned to avoid infinite weights.

In this study, both SPEI and SPI were calculated automatically using the SPEI package in R statistical software at 3-month and 12-month time scales to get a complete picture of the drought occurrences in the study area.

3 Results

The semi-arid regions of Iran stretch from the southeast to the northwest based on the Köppen climate classification. There are about 25 provinces lying in semi-arid regions in Iran. Several provinces have only small portions of their areas with semi-arid weather conditions. The SPI and SPEI in Iran are different from one place to another because Iran has two different semi-arid regions, which are known as cold and hot semi-arid regions.

3.1 Temporal and spatial analysis of the PDSI in semi-arid regions of Iran

The PDSI is separated into two different semi-arid regions based on cold and hot semi-arid weather. Figures 2 and 3 showed that cold semi-arid regions have lower PDSI range values (from 2.5 to –5.0 in most provinces) than hot semi-arid regions, which means that dry years are less in cold semi-arid regions compared to hot semi-arid regions. In almost all hot semi-arid regions, extreme dry occurred from 2000 to 2003 and from 2007 to 2014. In contrast, several areas in cold semi-arid regions only experienced moderate to severe dry from 2000 to 2003, except in West

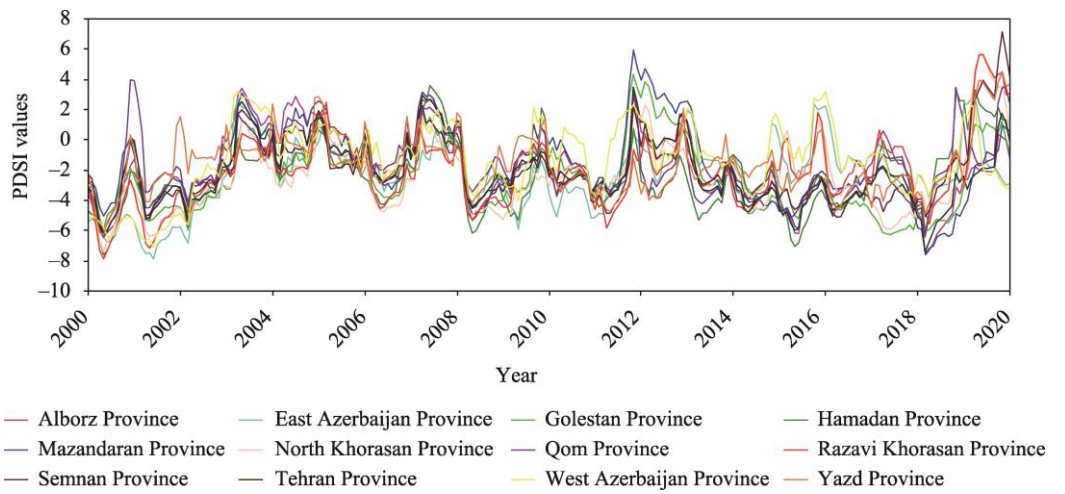

Fig. 2 Average Palmer Drought Severity Index (PDSI) values in cold semi-arid regions of Iran

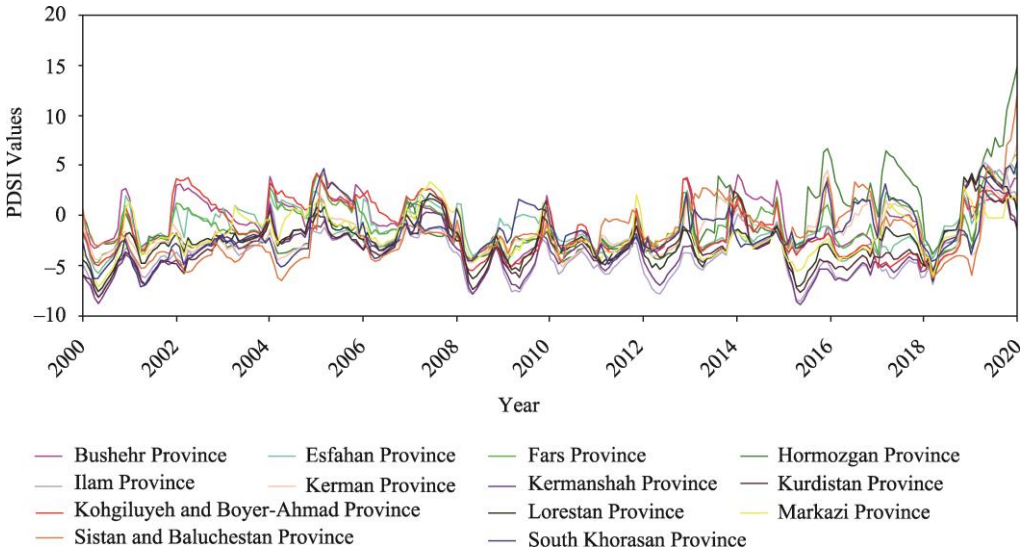

Fig. 3 Average PDSI values in hot semi-arid regions of Iran

Azerbaijan and North Khorasan provinces, which experienced extreme dry. In contrast, extreme wet conditions occurred in 2019, approximately in all hot semi-arid and cold semi-arid regions of Iran.

Simply, semi-arid regions in both East Azerbaijan and West Azerbaijan provinces are different from other provinces in the southeast and southwest semi-arid regions, in terms of dry years. For instance, unlike other cold semi-arid regions, a drought occurred in 2020. Although Mazandaran Province had several dry years, for example, in 2008 and during 2000–2003 and 2014–2018, compared to other provinces, it had many wet years because it lies south of the Caspian Sea, which leads to more precipitation. Razavi Khorasan Province fluctuated from severe dry to moderate dry in almost all years because precipitation fluctuated between 200 and 350 mm, as shown in Figure 1, except in 2019 and 2020, which recorded high precipitation and wet years. Moreover, several provinces may experience different drought from cold semi-arid and hot semi-arid regions, due to these provinces locate in both cold semi-arid and hot semi-arid regions, such as Esfahan, Fars, Hamadan, Hormozgan, Kerman, Markazi, Sistan and Baluchestan, and South Khorasan provinces. Furthermore, it is noticed that drought was more frequent in some provinces such as Razavi Khorasan, South Khorasan, Kerman, Fars, Esfahan, Semnan, Sistan and Baluchestan, and Lorestan provinces because these provinces had less precipitation, specifically, Razavi Khorasan, Semnan, Esfahan, South Khorasan, Yazd, and Kerman provinces (Figs. 2 and 3).

3.2 Different time scales of the SPI and the SPEI

3.2.1 SPI at 3-month time scale and SPEI at 3-month time scale

The monthly characteristics of both SPI at 3-month time scale (SPI-3) and SPEI at 3-month time scale (SPEI-3) fluctuated, which shows the variation of dry and wet conditions from one month to another month. The SPEI-3 and the SPI-3 dramatically fluctuated in approximately the same way in most semi-arid regions (Figs. 4 and S1). However, the SPEI-3 was slightly different in several years, which is due to the fact that the SPEI requires more data, such as evapotranspiration and temperature, resulting in different values in certain years. Also, evapotranspiration and temperature change with seasons, and there was variation in the SPEI values from one year to another year. The SPI-3 exceeded –2.0, which is known as extremely dry, in both Alborz and East Azerbaijan provinces in different years (2008, 2011, and 2018). Moreover, the SPEI-3 was negatively higher than the SPI-3 in 2019 in Alborz Province due to high temperature and potential evapotranspiration. Moreover, the SPEI-3 was positively high in several provinces in 2019

including Bushehr, Fars, Ilam, Kermanshah, Kohgiluyeh and Boyer-Ahmad, Markazi, Lorestan, and Qom provinces, due to low evapotranspiration and increased precipitation. Nevertheless, the SPI-3 was high or equal in value to the SPEI-3 in all semi-arid regions in both positive and negative directions (Fig. 4).

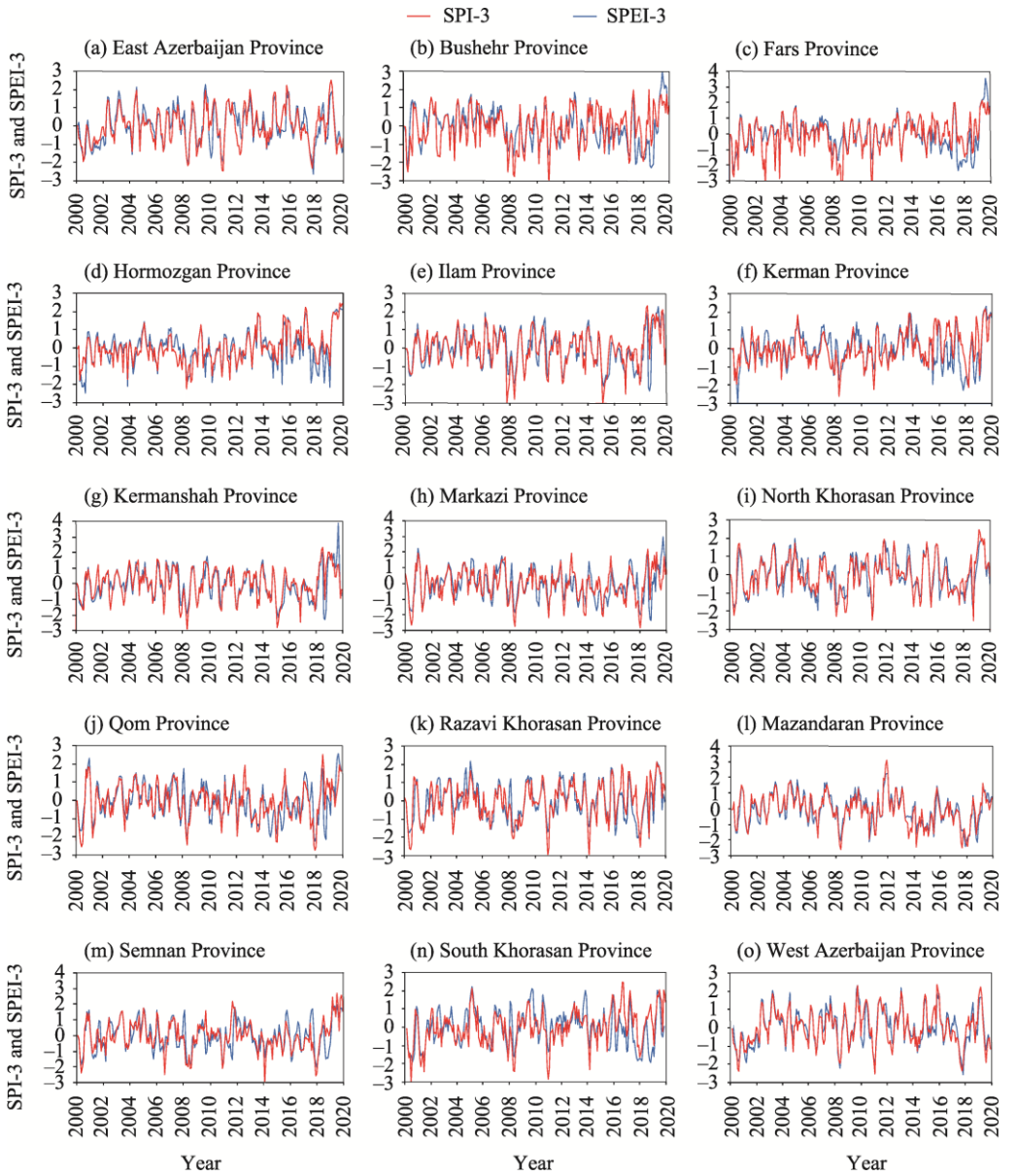

Fig. 4 Standard Precipitation Index (SPI) at 3-month time scale (SPI-3) and Standardized Precipitation Evapotranspiration Index (SPEI) at 3-month time scale (SPEI-3) in several semi-arid regions of Iran during 2000–2020. (a), East Azerbaijan Province; (b), Bushehr Province; (c), Fars Province; (d), Hormozgan Province; (e), Ilam Province; (f), Kerman Province; (g), Kermanshah Province; (h), Markazi Province; (i), North Khorasan Province; (j), Qom Province; (k), Razavi Khorasan Province; (l), Mazandaran Province; (m), Semnan Province; (n), South Khorasan Province; (o), West Azerbaijan Province.

In many semi-arid regions of Iran, the SPI-3 was higher than the SPEI-3 in 2000, 2008, 2014, 2015, and 2018. However, the entire semi-arid region was recorded as extremely dry in 2000. Although the SPEI-3 was lower than the SPI-3 or had the same values throughout the study periods, the SPEI-3 surpassed the SPI-3 in Hormozgan, Fars, Bushehr, Kerman, Kohgiluyeh and

Boyer-Ahmad, and South Khorasan provinces from 2016 to 2018, due to high evapotranspiration. In addition, several provinces experienced the same condition of high SPEI-3 in 2018 and 2020, for instance, East Azerbaijan, West Azerbaijan, Ilam, Kermanshah, Markazi, Lorestan, Mazandaran, Qom, Semnan, Tehran, and Yazd provinces (Figs 4 and S1).

Kerman Province had the highest SPEI-3 in the entire study area in 2000, due to the lowest precipitation and high temperature in this province. Meanwhile, reversed values were recorded in both SPI-3 and SPEI-3 in certain years. For instance, the positive SPI-3 and the negative SPEI-3 were recorded in several provinces, such as Fars, Kerman, and Hormozgan provinces. It indicated these provinces experienced high temperature even though sufficient precipitation was received in the same year. Also, both SPEI-3 and SPI-3 showed a 3-month lag, which means seasonal drought characteristics, which lead to negative and positive fluctuation values in approximately all years. Therefore, dry and wet conditions were witnessed in almost all years. Most importantly, for a few years, it exceeded –2.0, which is considered an extremely dry condition.

3.2.2 SPI at 12-month time scale and SPEI at 12-month time scale

Figure 5 illustrated the SPI-12 and the SPEI-12 in semi-arid regions of Iran. There are noticeably small differences seen in both indices because the SPEI-12 has considered evapotranspiration as a factor in drought impacts. If the SPEI-12 has a greater negative value, which means that evapotranspiration is high because of the high temperature. In contrast, if the SPEI has a greater positive value, which means that the region receives sufficient precipitation and, simultaneously, the temperature is low. For example, in 2001, 2017, and 2018, the SPEI-12 is a negative value in several regions, which means that evapotranspiration is high. In general, several major dry years that occurred in semi-arid regions, for instance, 2000–2003, 2007, 2009, 2011, 2014, 2015, and 2018. All semi-arid regions might not reflect drought in the same way due to semi-arid regions including two different climate zones, which are called cold semi-arid and hot semi-arid zones. Therefore, slight differences occurred from the southeast to the northwest. The SPEI-12 was a bit higher compared to the SPI-12 in several provinces from 2000 to 2003, including Alborz, Esfahan, Golestan, Hamadan, Ilam, Kermanshah, Lorestan, Markazi, Mazandaran, North Khorasan, Semnan, and Tehran provinces, which clearly shows that these provinces experienced high evapotranspiration as a result of increased temperature. Nevertheless, moderate and severe dry occurred in almost all semi-arid regions during 2001–2002, except West Azerbaijan, East Azerbaijan, Razavi Khorasan, and South Khorasan provinces, which had extremely dry years based on the both indices. Similarly, –2.0 was recorded in the both indices in all provinces since 2008. However, the SPEI-12 and the SPI-12 showed extreme and severe dry years during 2010–2011 in almost all study areas, except Mazandaran Province, due to their location in the Caspian Sea. The SPEI-12 was higher than the SPI-12 in 2008 in Hormozgan Province because it is also located in the Persian Gulf, where its temperature is very high. The driest year in Bushehr Province was 2010 and 2011 based on the SPI-12, due to a precipitation deficit. Furthermore, in the last decade, there were several periods in the semi-arid regions experienced severe to extreme dry in 2013 and during 2015–2016 and 2017–2018. In addition, extreme dry hit several provinces, including Mazandaran, Ilam, Lorestan, Kermanshah, Qom, and Tehran provinces in 2015.

Moreover, the SPEI-12 showed extreme dry in Hormozgan, Kerman, Fars, South Khorasan, and North Khorasan provinces during 2017–2018. Simultaneously, the SPI-12 showed moderate dry in these provinces, which means that the high temperature was dominant in these provinces, which has high SPEI-12. Alborz Province was extremely dry in 2009 and 2018 and severe dry in 2001, 2003, and 2015 (Fig. S2). Furthermore, moderate dry years were frequent, which were recorded in both indices, and longer dry years occurred from 2000 to 2003 and from 2014 to 2018 in some regions in semi-arid regions of Iran. Most importantly, dryness was more occurred between 2010 and 2020 compared to from 2000 to 2010. This indicated that it spreads across most areas in the region, and precipitation variability is not significant among these places.

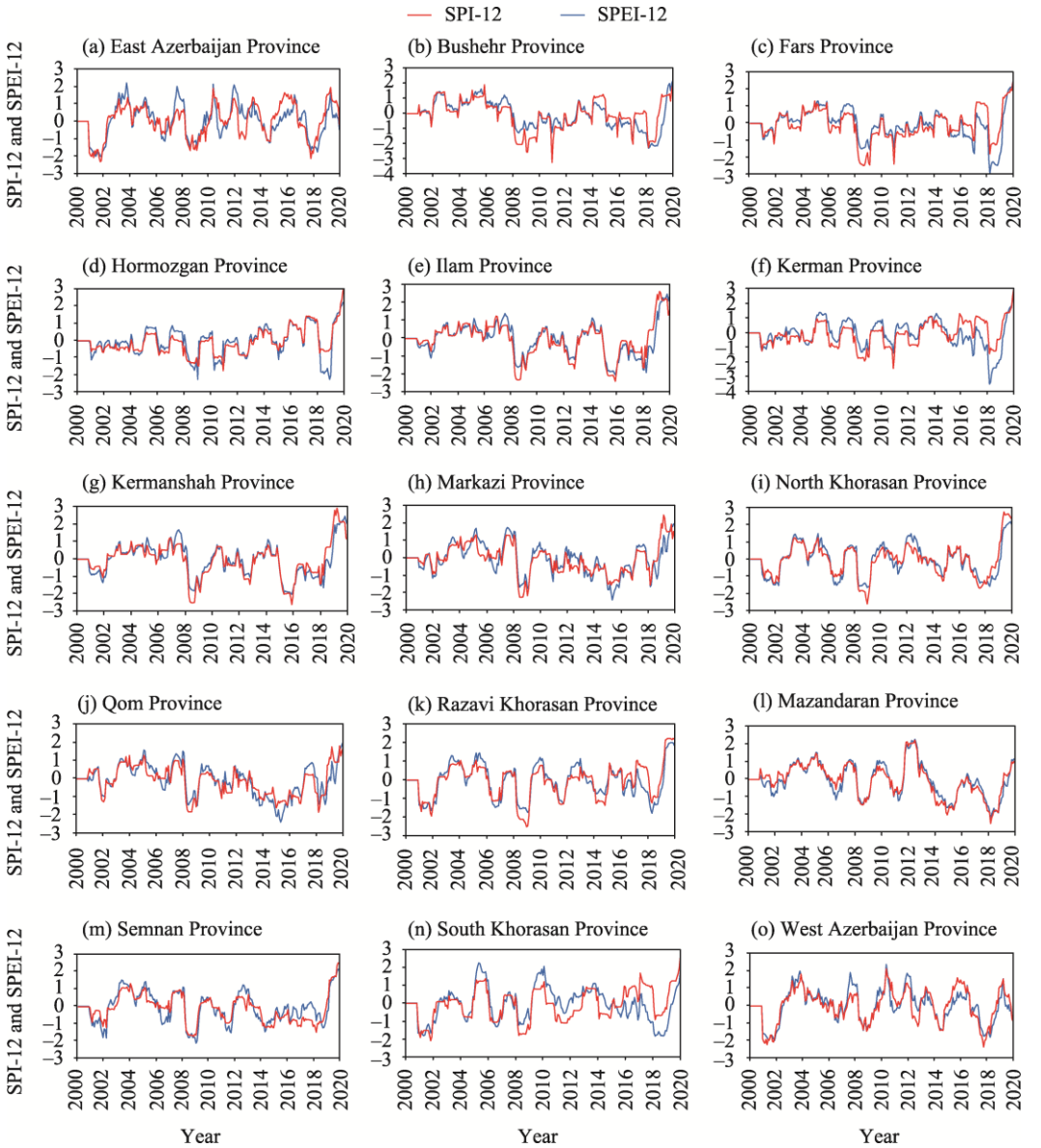

Fig. 5 SPI at 12-month time scale (SPI-12) and SPEI at 12-month time scale (SPEI-12) in several semi-arid regions of Iran during 2000–2020. (a), East Azerbaijan Province; (b), Bushehr Province; (c), Fars Province; (d), Hormozgan Province; (e), Ilam Province; (f), Kerman Province; (g), Kermanshah Province; (h), Markazi Province; (i), North Khorasan Province; (j), Qom Province; (k), Razavi Khorasan Province; (l), Mazandaran Province; (m), Semnan Province; (n), South Khorasan Province; (o), West Azerbaijan Province.

3.3 Frequency of dry and wet periods

Analyzing the periods of dry and wet events in the last 20 years, it was found that both SPI-12 and SPEI-12 are approximately similar in the extent of dry and wet months. Figure 6 showed that most of the provinces have normal weather conditions, but several provinces recorded slightly lower frequencies of normal conditions, such as Kermanshah, Bushehr, and Kurdistan provinces, instead they witnessed higher moderate wet periods. This is due to these provinces received higher precipitation compared to other provinces in the same climatic zone. In contrast, although extreme dry has reached its lowest values in most of the provinces, several provinces have still displayed slightly extreme dry compared to others, such as Esfahan, Fars, Kohgiluyeh and Boyer-Ahmad, and Markazi provinces. According to the SPI-3, the second highest periods in the

regions were moderate wet and dry. Figure 6b showed the SPEI-3 in semi-arid regions that near normal regions was the highest value, while moderate wet and dry were the second highest values in all provinces. Figure 6b and c showed that near normal was also a highest value in both indices. In addition, Figure 6c and d illustrated both extreme wet and dry classes were slightly higher in several places than other semi-arid regions. Despite of dry and wet conditions were witnessed in almost all years.

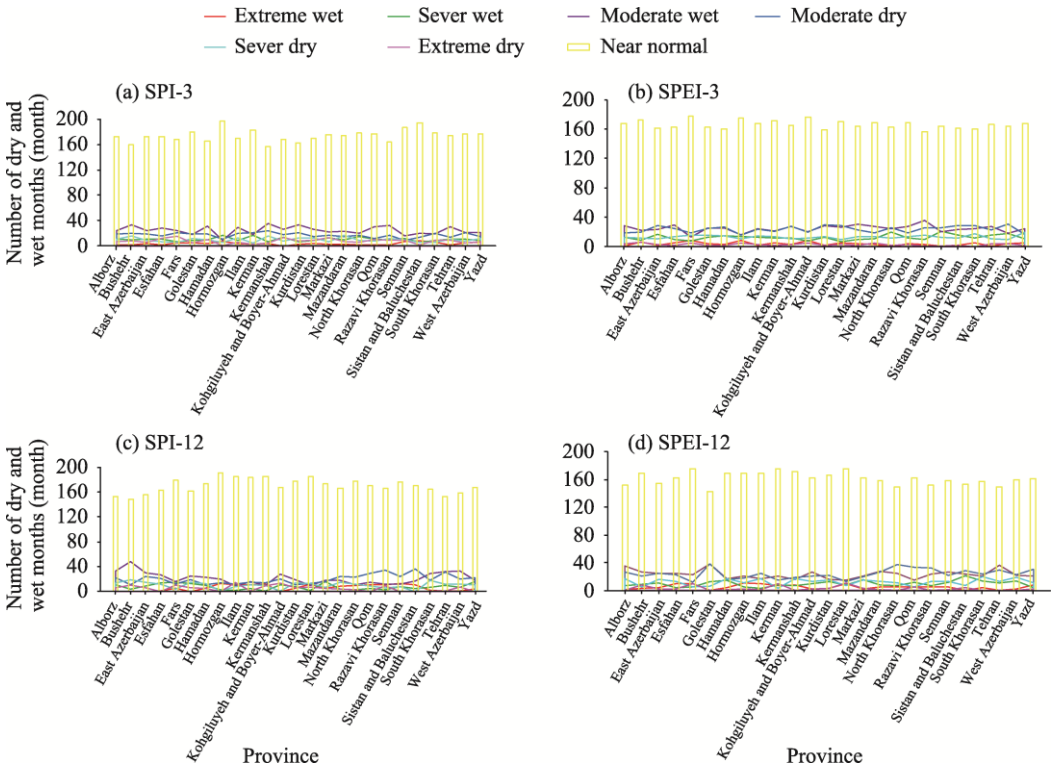

Fig. 6 Number of dry and wet months in semi-arid regions of Iran based on SPI-3 (a), SPEI-3 (b), SPI-12 (c), and SPEI-12 (d) during 2000–2020

3.4 Drought events analysis based on spatial distribution of the SPEI and the SPI

The spatial distribution is conducted in both winter and summer seasons, as well as wet and dry seasons for detecting drought. Although drought is not specific to one season, it is significant to display dry and wet conditions in two seasons, such as winter and summer, in semi-arid regions of Iran. Therefore, both seasons could reveal drought in the region. The map of SPI-12 showed that the region has undergone noticeably normal conditions in general. For several years, there was a moderate to severe dry. For instance, moderate dry was recorded in the winter of 2002 in several provinces, such as Razavi Khorasan, North Khorasan, Qom, West Azerbaijan, and East Azerbaijan provinces, and again in the summer of 2012 in Kermanshah and Ilam provinces. Severe and moderate dry happened in 2015 and 2017 in North and Southwest Iran. Most of the dry seasons occurred in the North and Southwest Iran due to a lack of sufficient precipitation. The wettest season was in the winter of 2020, which was the wettest recorded in the last 20 years, even though it started at the beginning of 2019 (Fig. S3). While the map of SPEI-12 indicated that near normal, moderate dry, severe dry, moderate wet, and severe wet conditions have occurred in several years (Fig. S4). Moderate dry to severe dry conditions were recorded in 2002 in East and Northeast Iran, including Kerman, Sistan and Baluchestan, Semnan, Razavi Khorasan, North Khorasan, Tehran, and Kermanshah provinces; extremely dry conditions occurred in West Azerbaijan and East Azerbaijan provinces. In addition, moderate wet conditions occurred for several years, such as 2002 in Southwest Iran, 2007 in Southeast and Northwest Iran, and 2012 in North Iran.

In 2015, moderate dry to severe dry was detected in both seasons in northwest provinces, which started from Mazandaran Province to Kermanshah Province in West Iran, except in West Azerbaijan and East Azerbaijan provinces. In the summer, a severe drought hit Sistan and Baluchistan and Kerman provinces. In 2017, moderate dry happened sparsely in the region, but the biggest part of moderate dry and severe dry was seen in the summer in Southwest Iran, which includes Fars, Bushehr, and Kohgiluyeh and Boyer-Ahmad provinces. It continued into the winter of 2019, especially in Southeast Iran, whereas wet condition was shown in different years, such as in 2005, 2007, 2010, 2012, 2019, and 2020.

4 Discussion

Three indices are used for identifying meteorological drought in semi-arid regions of Iran, such as SPI, SPEI, and PDSI. The PDSI was used to identify meteorological drought in several studies (Dash et al., 2012; Dehghan et al., 2020; Tao and Zhang 2020). The PDSI, where the main variables are weather data, which is suitable for detecting drought in longer periods. Since it is designed in a way that considers average monthly data, which depends on the principle of the rate of balance between both supply and demand for moisture (Karl, 1983). Drought based on the PDSI is frequent and occurs in all semi-arid regions of Iran. Negative values, which are considered dry weather, occurred from 2000 to 2004 in all semi-arid regions equally with low precipitation and high temperature, which is similar to the previous two studies (Darand, 2015; Kheyri et al., 2021) that used the PDSI for drought monitoring, and confirmed that Iran experienced a dry period between 2000 and 2004. However, it is also similar to the study that was conducted in Ardebil Province in the northwest of Iran by Kazemzadeh and Malekian (2016), which detected meteorological drought during 2000–2004, 2007–2008, and 2010–2010 based on the SPI. In this study, a meteorological drought occurred in 2008 and during 2010–2011 and 2014–2018, from Hamadan and Qom provinces in the cold semi-arid regions to Lorestan, Esfahan, Fars, Markazi, Kermanshah, Kohgiluyeh and Boyer-Ahmad, Razavi Khorasan, and Semnan provinces in the hot semi-arid regions. The result is the same as a study conducted in Fars Province of Iran (Dehghan et al., 2020), which showed that 2000–2001, 2008, and 2010 had a drought and predicted for increasing drought after 2014. Another study, which was consistent with the results of this study, recorded the same dry years and precipitation deficit in 2000, 2001, 2008, and 2010 in Fars Province (Hossein et al., 2014). From 2008 to 2018, the same drought periods affected Golestan, Yazd, and Tehran provinces, except from 2012 to 2013.

The SPEI and SPI are both used for drought variation and monitoring, but the SPI neglects the impacts of evaporation on drought, whereas the SPEI is applied to both precipitation and evapotranspiration because the SPEI is an appropriate method for semi-arid regions. Both SPI and SPEI varied often around the value of 0.0, with a huge range due to the influence of short-term climatic change, which may clearly show the subtle shift in water profit and loss at 3-month time scale (Pei et al., 2020). This study showed that the semi-arid regions underwent normal conditions of weather from 2000 to 2020. For example, moderate dry, severe dry, and extreme dry occurred with a lower percentage in a way that gradually decreased. For instance, moderate dry has a higher percentage than both severe dry and extreme dry in almost all the places in semi-arid regions in the both SPI and SPEI. Therefore, similar research conducted by Bari Abarghouei et al. (2011) demonstrated an increasing severity of meteorological drought based on the SPI, and also another study had the same result with an increased meteorological drought based on the Reconnaissance Drought Index (Kousari et al., 2014). Although both extreme dry and extreme wet had the lowest percentage in both indices, extreme dry and extreme wet rarely happened in the SPEI-12 and the SPI-12, respectively, due to the use of climatic characteristics. According to the calculated SPEI values, the normal class of drought severity had the maximum occurrence frequency (approximately 60%–70% during the studied years), and extreme wet had the lowest occurrence frequency (less than 2% during the studied years) in all stations and at all time scales. The estimated SPI values revealed that the SPI-based results for the occurrence frequency of

different classes of drought severity were nearly identical to those of the SPEI (Zarei et al., 2021). Both indices on different scales showed that they do not significantly vary from each other in almost all regions in this study, which is similar to the study that was conducted by Sharafati et al. (2020). The results showed high agreement between the SPI and the SPEI, indicating that meteorological drought in Iran is more responsive to precipitation than potential evapotranspiration. The excellent correlations also implied that the results obtained in this study using the SPI would not differ if a similar analysis was performed using the SPEI. However, the SPEI was higher than the SPI in several regions in different years, which is a sign of high potential evapotranspiration in those areas, especially in 2018. Therefore, Zarei et al. (2021 mentioned that potential evapotranspiration was high in some provinces due to high temperature and low precipitation.

Spatial distribution is the most important key to evaluate drought events visually, and it is a widespread technique to understand the drought phenomenon and is widely acknowledged by drought professionals (Andreadis et al., 2005; Guo et al., 2017). In this study, both SPEI and SPI are considered to be the optimum to show specific drought because whenever the SPI is computed at short periods in regions with minimal seasonal precipitation, it might cause huge positive or negative results, which could be misleading (Sönmez et al., 2005; World Meteorological Organization., 2012; Guo et al., 2017). In the SPI-3, normal conditions are great in all years except in 2000, 2008, 2012, 2015, and 2017, which is the same as the study conducted by Zarei et al. (2017). A previous study conducted in the central and southern parts of Iran illustrated that most of semi-arid regions, where are prone to high drought frequencies likely to suffer drought with returned periods between 5 to 10 years, based on the SPI-12 (Alijanian et al., 2019). The current study showed that drought did not occur in all regions in the same year. It only happened in specific regions of Iran because the precipitation and evapotranspiration were not the same as shown in Figures S3 and S4. Although moderate dry to extreme dry occurs in almost all years, not in all semi-arid regions, it affects only specific areas. The normal drought dominates most of the semi-arid regions.

Contrary to our results, a study conducted by Nasrollahi et al. (2018) illustrated that moderate dry and severe dry have the highest percentages in Semnan Province. Furthermore, the SPEI normal class was the highest value and extreme class as the lowest value, which is consistent with a study conducted by Zarei et al. (2021) that demonstrated that normal class was the highest value and extreme wet class was the lowest value. Nejadrekabi et al. (2022) conducted a study in Khuzestan Province on the border of our study area and found that the severity of the drought has increased since 2012 and the drought hit the southern and southeastern parts of Khuzestan Province based on the SPEI. It is found that in the summer of 2017 and the winter of 2019, a drought occurred in near Khuzestan Province. Finally, our results are nearly consistent with a study carried out by Karakani et al. (2021), which used the SPI and illustrated that the Middle East underwent near-normal conditions in most of years between 2001 and 2017, but 2001, 2006, and 2008 were recorded as moderate dry.

5 Conclusions

Drought is a serious natural hazard that occurs in practically all climates. TerraClimate was used as an alternative to station data to show drought in semi-arid regions of Iran, which are considered the largest semi-arid regions in the world. The PDSI findings showed that cold semi-arid regions have the lower PDSI range values than hot semi-arid regions, which range from 2.5 to –5.0 in most regions. It means that the semi-arid regions underwent normal conditions of weather from 2000 to 2020. Moderate, severe, and extreme dry occurred with a lower percentage in a way that gradually decreased respectively. For example, moderate dry has a higher percentage than severe dry and extreme dry in almost all the areas in semi-arid regions. According to the SPI-12 and the SPEI-12, the years with moderate dry are frequently recorded in both indices, and the longest dry years occurred from 2000 to 2003 and from 2014 to 2018 in most areas in semi-arid regions.

Moreover, years with extreme dry and severe dry are recorded in 2007, 2008, 2011, and 2017. According to the spatial distribution of the SPEI and the SPI, the semi-arid regions have experienced near-normal conditions in general. However, it is determined that TerraClimate data is suitable to be an alternative for the areas where *in-situ* data is unfeasible, especially for desert, arid, and semi-arid weather in a future study.

Acknowledgements

We thank the TerraClimate Database for such outstanding global climate data products as well as the Google Earth Engine platform for using them in some parts of this research. Many thanks to the editors and reviewers for their thoughtful comments.

References

Abatzoglou J T, Dobrowski S Z, Parks S A, et al. 2018a. TerraClimate, a high-resolution global dataset of monthly climate and climatic water balance from 1958–2015. [2022-05-01]. https://www.climatologylab.org/TerraClimate.html.

Abatzoglou J T, Dobrowski S Z, Parks S A, et al. 2018b. TerraClimate, a high-resolution global dataset of monthly climate and climatic water balance from 1958–2015. Scientific Data, 5: 170191, doi: 10.1038/sdata.2017.191.

Abatzoglou J T, Dobrowski S Z, Parks S A, et al. 2021. TerraClimate Individual years for +2C and +4C climate futures. [2022-09-08]. https://samapriya.github.io/awesome-gee-community-datasets/projects/terraclim/.

Abdelmigid H M, Baz M, AlZain M A, et al. 2022. Spatiotemporal deep learning model for prediction of Taif Rose phenotyping. Agronomy, 12(4): 807, doi: 10.3390/agronomy12040807.

Alijanian M, Rakhshandehroo G R, Mishra A, et al. 2019. Evaluation of remotely sensed precipitation estimates using PERSIANN-CDR and MSWEP for spatio-temporal drought assessment over Iran. Journal of Hydrology, 579: 124189, doi: 10.1016/j.jhydrol.2019.124189.

Allen R G, Pereira L S, Raes D, et al. 1998. Crop evapotranspiration-guidelines for computing crop water requirements. In: FAO Irrigation & Drainage Paper No. 56. Rome, Italy.

Andreadis K M, Clark E A, Wood A W, et al. 2005. Twentieth-century drought in the conterminous United States. Journal of Hydrometeorology, 6(6): 985–1001.

Araneda R J, Puertas J, Maia R, et al. 2020. Unified framework for drought monitoring and assessment in a transboundaryriver basin. In: Uijttewaal W, Franca M, Valero D, et al. River Flow (1st ed.). London: CRC Press. 1081–1086.

Banimahd S A, Khalili D. 2013. Factors influencing Markov chains predictability characteristics, utilizing SPI, RDI, EDI and SPEI drought indices in different climatic zones. Water Resources Management, 27(11): 3911–3928.

Bari Abarghouei H, Asadi Zarch M A, Dastorani M T, et al. 2011. The survey of climatic drought trend in Iran. Stochastic Environmental Research and Risk Assessment, 25(6): 851–863.

Beyaztas U, Arikan B B, Beyaztas B H, et al. 2018. Construction of prediction intervals for Palmer Drought Severity Index using bootstrap. Journal of Hydrology, 559: 461–470.

Chen F W, Liu C W. 2012. Estimation of the spatial rainfall distribution using inverse distance weighting (IDW) in the middle of Taiwan. Paddy and Water Environment, 10(3): 209–222.

Darand M. 2015. Drought monitoring in Iran by palmer severity drought index (PDSI) and correlation with oceanic atmospheric teleconnection patterns. Geographical Research, 29(4): 67–82.

Dash B K, Rafiuddin M, Khanam F, et al. 2012. Characteristics of meteorological drought in Bangladesh. Natural Hazards, 64(2): 1461–1474.

Dehghan S, Salehnia N, Sayari N, et al. 2020. Prediction of meteorological drought in arid and semi-arid regions using PDSI and SDSM: a case study in Fars Province, Iran. Journal of Arid Land, 12(2): 318–330.

Guo H, Bao A M, Liu T, et al. 2017. Meteorological drought analysis in the Lower Mekong Basin using satellite-based long-term CHIRPS product. Sustainability, 9(6): 901, doi: 10.3390/su9060901.

Hamarash H R, Rasul A, Hamad R O, et al. 2022. A review of methods used to monitor and predict droughts. Preprints, 2022080539, doi: 10.20944/preprints202208.0539.v1.

Hamed M M, Nashwan M S, Shahid S. 2021. Performance evaluation of reanalysis precipitation products in Egypt using fuzzy entropy time series similarity analysis. International Journal of Climatology, 41(11): 5431–5446.

Hossein Z L, Reza F H, Fardin B. 2014. Evaluation of the wheat agricultural drought return period in the province of Fars using RDI index. Journal of Water Resources Engineering, Islamic Azad University, 7(22): 1–10.

Huerta A, Lavado W, Rau P. 2020. The vulnerability of water availability in Peru due to climate change: A probabilistic Budyko

analysis. [2022-09-08]. https://ui.adsabs.harvard.edu/abs/2020EGUGA.22.3766H/abstract.

Karakani E G, Malekian A, Gholami S, et al. 2021. Spatiotemporal monitoring and change detection of vegetation cover for drought management in the Middle East. Theoretical and Applied Climatology, 144(1): 299–315.

Karl T R. 1983. Some spatial characteristics of drought duration in the United States. Journal of Applied Meteorology and Climatology, 22(8): 1356–1366.

Kazemzadeh M, Malekian A. 2016. Spatial characteristics and temporal trends of meteorological and hydrological droughts in northwestern Iran. Natural Hazards, 80(1): 191–210.

Kheyri R, Mojarrad F, Masompour J, et al. 2021. Evaluation of drought changes in Iran using SPEI and SC-PDSI. The Journal of Spatial Planning, 25(1): 175–206.

Kodandapani N, Parks S A. 2019. Effects of drought on wildfires in forest landscapes of the Western Ghats, India. International Journal of Wildland Fire, 28(6): 431–444.

Kousari M R, Dastorani M T, Niazi Y, et al. 2014. Trend detection of drought in arid and semi-arid regions of Iran based on implementation of reconnaissance drought index (RDI) and application of non-parametrical statistical method. Water Resources Management, 28(7): 1857–1872.

Liu C H, Yang C P, Yang Q, et al. 2021. Spatiotemporal drought analysis by the standardized precipitation index (SPI) and standardized precipitation evapotranspiration index (SPEI) in Sichuan Province, China. Scientific Reports, 11: 1280, doi: 10.1038/s41598-020-80527-3.

Martinez-Villalobos C, Neelin J D. 2019. Why do precipitation intensities tend to follow gamma distributions? Journal of the Atmospheric Sciences, 76(11): 3611–3631.

McKee T B, Doesken N J, Kleist J. 1993. The relationship of drought frequency and duration to time scales. In: Proceedings of the 8th Conference on Applied Climatology. Boston, USA.

Nasrollahi M, Khosravi H, Moghaddamnia A, et al. 2018. Assessment of drought risk index using drought hazard and vulnerability indices. Arabian Journal of Geosciences, 11: 606, doi: 10.1007/s12517-018-3971-y.

Nejadrekabi M, Eslamian S, Zareian M J. 2022. Spatial statistics techniques for SPEI and NDVI drought indices: A case study of Khuzestan Province. International Journal of Environmental Science and Technology, 19: 6573–6594.

Neto A K, Ribeiro R B, Pruski F F. 2022. Assessment water balance through different sources of precipitation and actual evapotranspiration. [2022-09-08]. https://doi.org/10.21203/rs.3.rs-1443692/v1.

Palmer W C. 1965. Meteorological Drought. Washington: Office of Climatology, US Weather Bureau, 7–12.

Peel M C, Finlayson B L, McMahon T A. 2007. Updated world map of the Köppen-Geiger climate classification. Hydrology and Earth System Sciences, 11(5): 1633–1644.

Pei Z F, Fang S B, Wang L, et al. 2020. Comparative analysis of drought indicated by the SPI and SPEI at various timescales in Inner Mongolia, China. Water, 12(7): 1925, doi: 10.3390/w12071925.

Rahimi J, Laux P, Khalili A. 2020. Assessment of climate change over Iran: CMIP5 results and their presentation in terms of Köppen–Geiger climate zones. Theoretical and Applied Climatology, 141(1): 183–199.

Salvacion A R. 2022. Multiscale drought hazard assessment in the Philippines. Computers in Earth and Environmental Sciences, doi: 10.1016/B978-0-323-89861-4.00024-5.

Sharafati A, Nabaei S, Shahid S. 2020. Spatial assessment of meteorological drought features over different climate regions in Iran. International Journal of Climatology, 40(3): 1864–1884.

Sönmez F K, Koemuescue A U, Erkan A, et al. 2005. An analysis of spatial and temporal dimension of drought vulnerability in Turkey using the standardized precipitation index. Natural Hazards, 35(2): 243–264.

Tall A. 2008. Application of the palmer drought severity index in east Slovakian lowland. Cereal Research Communications, 36: 1195–1198.

Tan C P, Yang J P, Li M. 2015. Temporal-spatial variation of drought indicated by SPI and SPEI in Ningxia Hui Autonomous Region, China. Atmosphere, 6(10): 1399–1421.

Tao R, Zhang K, 2020. PDSI-based analysis of characteristics and spatiotemporal changes of meteorological drought in China from 1982 to 2015. Water Resources Protection, 36(5): 50–56. (in Chinese with English abstract)

Tatli H, Türkeş M. 2011. Empirical orthogonal function analysis of the Palmer drought indices. Agricultural and Forest Meteorology, 151(7): 981–991.

Tefera A S, Ayoade J O, Bello N J. 2019. Comparative analyses of SPI and SPEI as drought assessment tools in Tigray Region, Northern Ethiopia. SN Applied Sciences, 1: 1265, doi: 10.1007/s42452-019-1326-2.

Vicente-Serrano S M, Beguería S, López-Moreno J I. 2010. A multiscalar drought index sensitive to global warming: the standardized precipitation evapotranspiration index. Journal of Climate, 23(7): 1696–1718.

Wang H J, Chen Y N, Pan Y P, et al. 2019. Assessment of candidate distributions for SPI/SPEI and sensitivity of drought to

climatic variables in China. International Journal of Climatology, 39(11): 4392–4412.

World Meteorological Organization. 2012. Standardized precipitation index user guide. In: Svoboda M, Hayes M, Wood D. World Meteorological Organization No. 1090. Geneva: World Meteorological Organization.

Yang P, Xia J, Zhang Y Y, et al. 2018. Comprehensive assessment of drought risk in the arid region of Northwest China based on the global palmer drought severity index gridded data. Science of the Total Environment, 627: 951–962.

Zarei A, Asadi E, Ebrahimi A, et al. 2017. Comparison of meteorological indices for spatio-temporal analysis of drought in Chahrmahal-Bakhtiyari province in Iran. Croatian Meteorological Journal, 52: 13–26.

Zarei A R, Shabani A, Moghimi M M. 2021. Accuracy assessment of the SPEI, RDI and SPI drought indices in regions of Iran with different climate conditions. Pure and Applied Geophysics, 178(4): 1387–1403.

Zhang J, Sun F B, Lai W L, et al. 2019. Attributing changes in future extreme droughts based on PDSI in China. Journal of Hydrology, 573: 607–615.

Zhang Y J, Yu Z S, Niu H S. 2018. Standardized Precipitation Evapotranspiration Index is highly correlated with total water storage over China under future climate scenarios. Atmospheric Environment, 194: 123–133.

Zhou Y L, Zhou P, Jin J L, et al. 2022. Drought identification based on Palmer drought severity index and return period analysis of drought characteristics in Huaibei Plain China. Environmental Research, 212: 113163, doi: 10.1016/j.envres.2022.113163.

Zoljoodi M, Didevarasl A. 2013. Evaluation of spatial-temporal variability of drought events in Iran using palmer drought severity index and its principal factors (through 1951–2005). Atmospheric and Climate Sciences, 3(2): 193–207.

Appendix

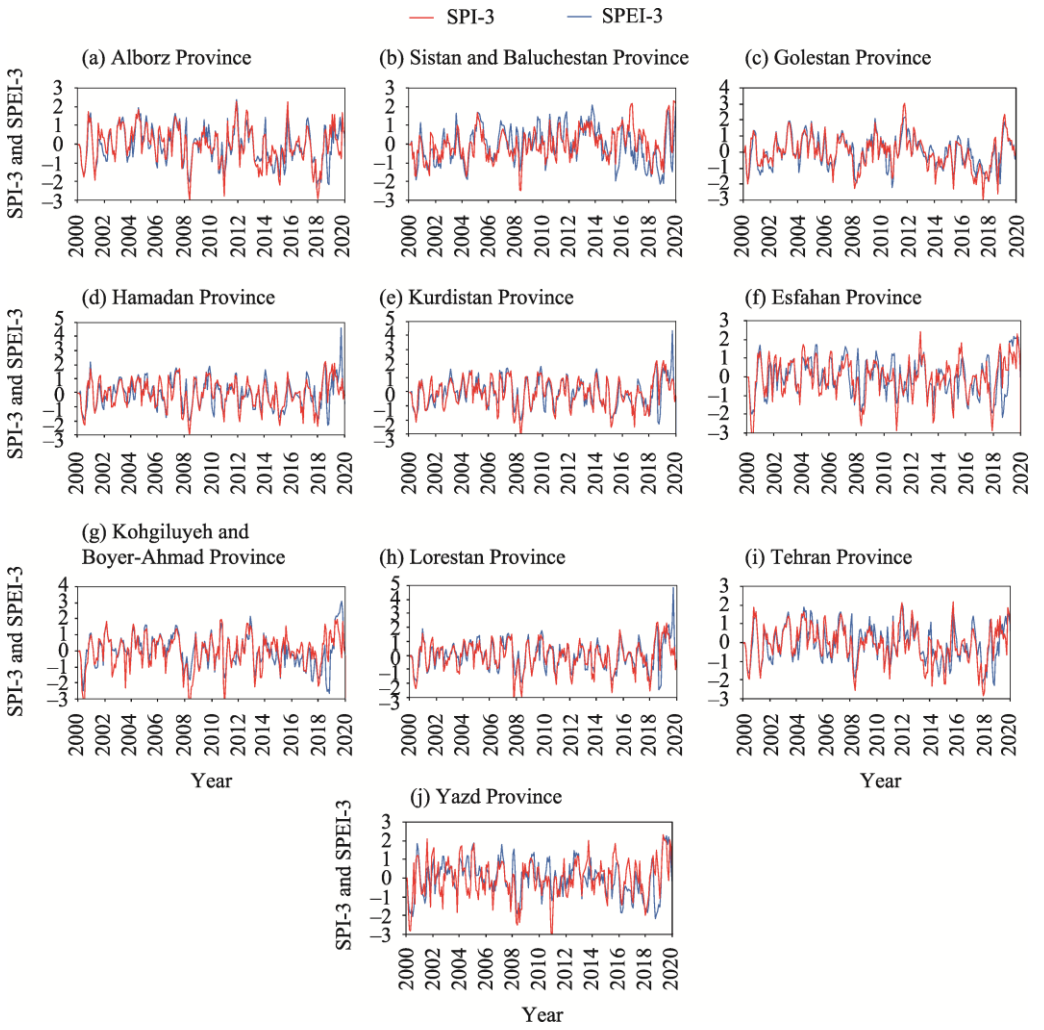

Fig. S1 Standard Precipitation Index (SPI) at 3-month time scale (SPI-3) and Standardized Precipitation Evapotranspiration Index (SPEI) at 3-month time scale (SPEI-3) in several semi-arid regions of Iran during 2000–2020. (a), Alborz Province; (b), Sistan and Baluchestan Province; (c), Golestan Province; (d), Hamadan Province; (e), Kurdistan Province; (f), Esfahan Province; (g), Kohgiluyeh and Boyer-Ahmad Province; (h), Lorestan Province; (i), Tehran Province; (j), Yazd Province.

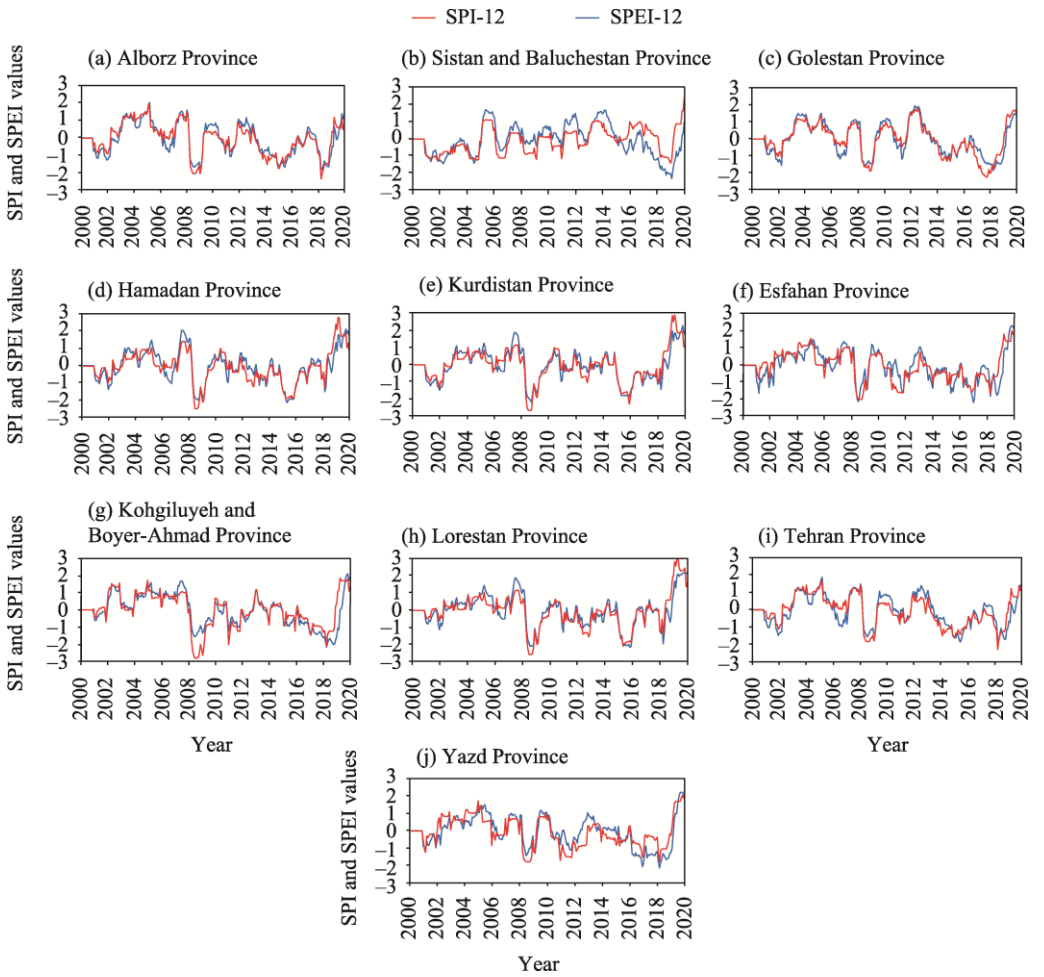

Fig. S2 SPI at 12-month time scale (SPI-12) and SPEI at 12-month time scale (SPEI-12) in several semi-arid regions of Iran during 2000–2020. (a), Alborz Province; (b), Sistan and Baluchestan Province; (c), Golestan Province; (d), Hamadan Province; (e), Kurdistan Province; (f), Esfahan Province; (g), Kohgiluyeh and Boyer-Ahmad Province; (h), Lorestan Province; (i), Tehran Province; (j), Yazd Province.

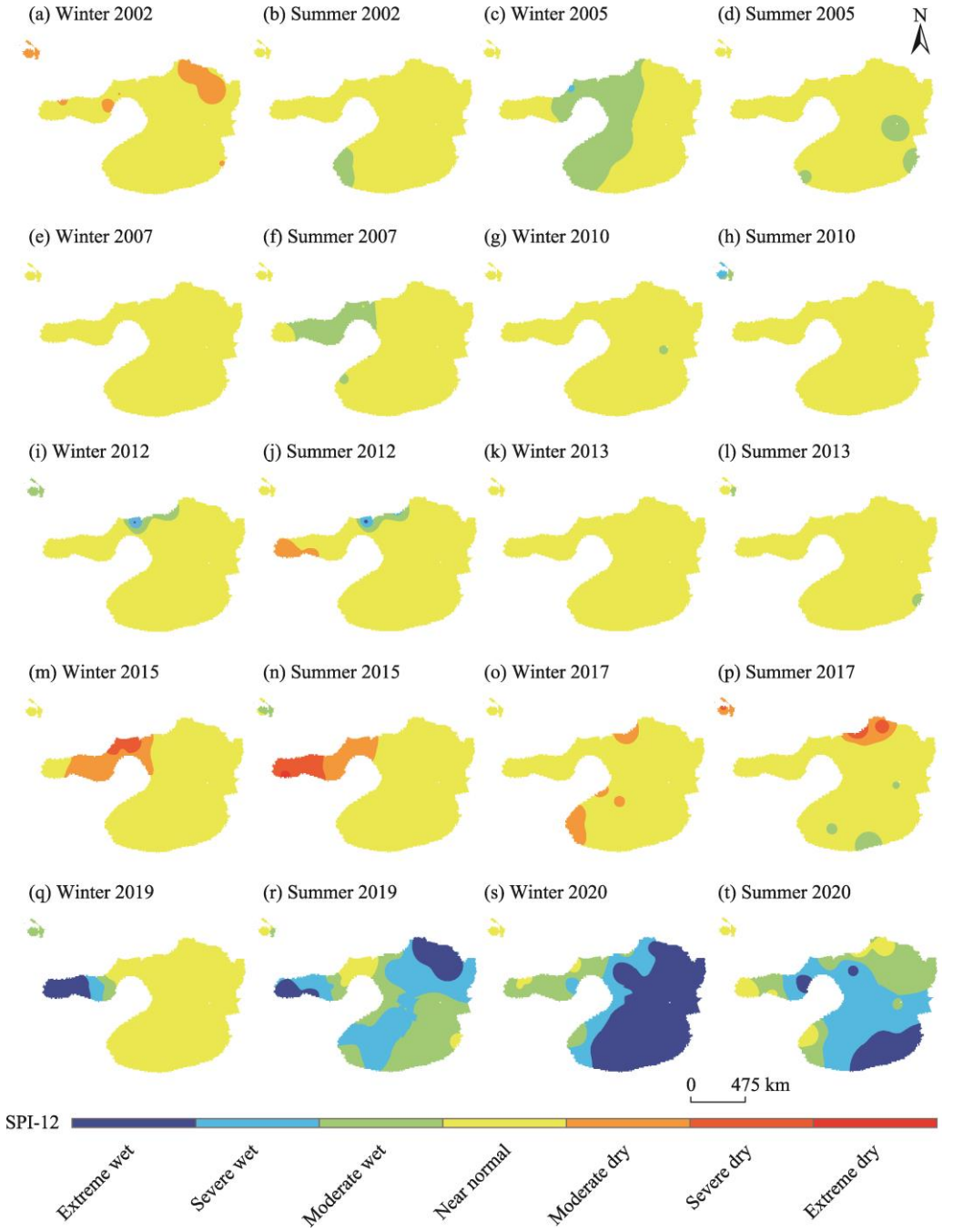

Fig. S3 Spatial and temporal distribution of SPI-12 in winter and summer in semi-arid regions of Iran. (a), Winter 2002; (b), Summer 2002; (c), Winter 2005; (d), Summer 2005; (e), Winter 2007; (f), Summer 2007; (g), Winter 2010; (h), Summer 2010; (i), Winter 2012; (j), Summer 2012; (k), Winter 2013; (l), Summer 2013; (m), Winter 2015; (n), Summer 2015; (o), Winter 2017; (p), Summer 2017; (q), Winter 2019; (r), Summer 2019; (s), Winter 2020; (t), Summer 2020.

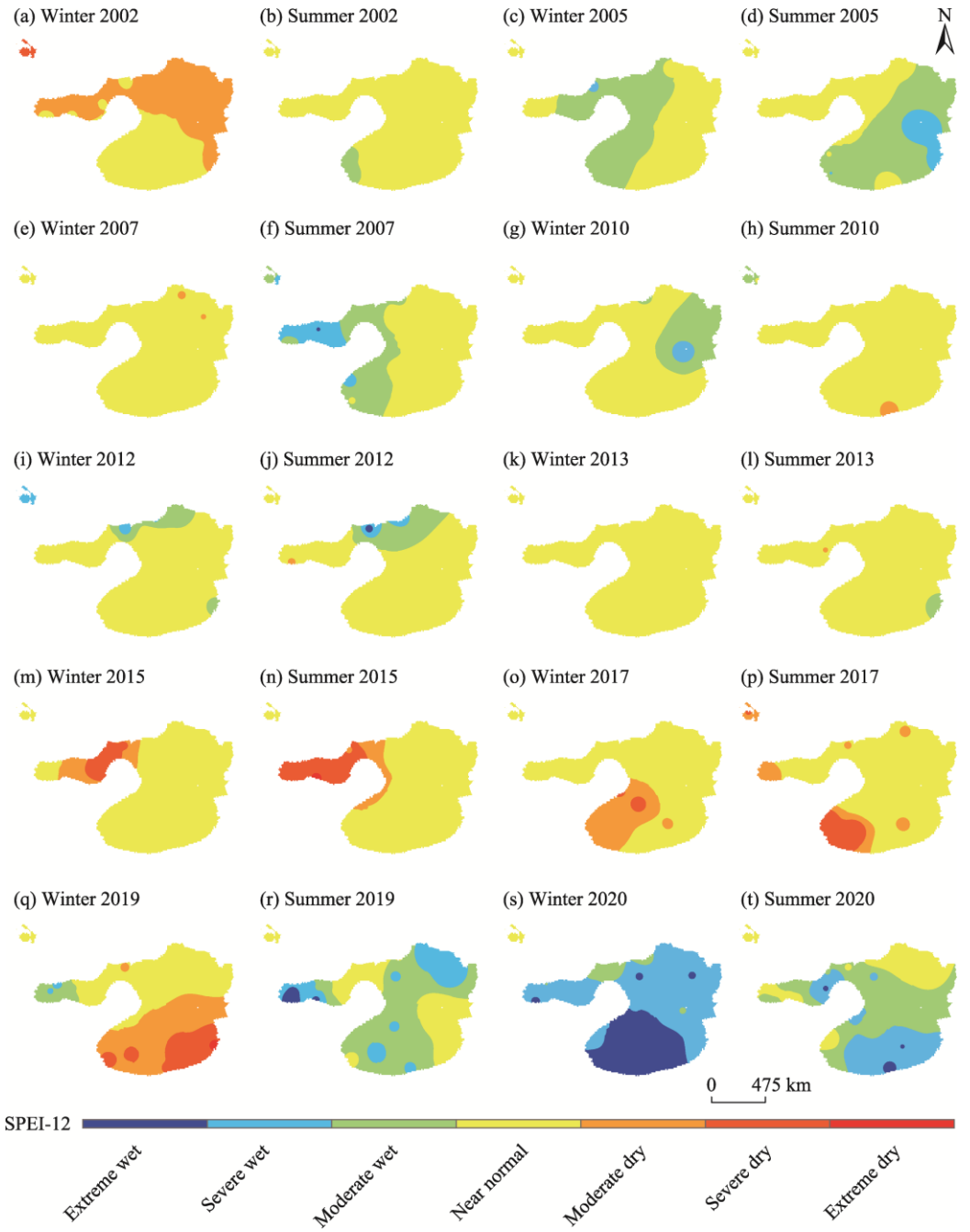

Fig. S4 Spatial and temporal distribution of SPEI-12 in winter and summer in semi-arid regions of Iran. (a), Winter 2002; (b), Summer 2002; (c), Winter 2005; (d), Summer 2005; (e), Winter 2007; (f), Summer 2007; (g), Winter 2010; (h), Summer 2010; (i), Winter 2012; (j), Summer 2012; (k), Winter 2013; (l), Summer 2013; (m), Winter 2015; (n), Summer 2015; (o), Winter 2017; (p), Summer 2017; (q), Winter 2019; (r), Summer 2019; (s), Winter 2020; (t), Summer 2020.